Applied Energy 112 (2013) 1087–1099

Contents lists available at SciVerse ScienceDirect

Applied Energy

journal homepage: www.elsevier.com/locate/apenergy

Comprehensive exergy-based evaluation and parametric study of a coal-fired ultra-supercritical power plant

Yongping Yang [a], Ligang Wang [a,b,*], Changqing Dong [a], Gang Xu [a], Tatiana Morosuk [b], George Tsatsaronis [b]

[a] School of Energy, Power and Mechanical Engineering, North China Electric Power University, Beinong Road 2, Beijing 102206, China
[b] Institut für Energietechnik, Technische Universität Berlin, Marchstraße 18, Berlin 10587, Germany

HIGHLIGHTS

- Detailed spatial distribution of exergy destruction and losses is provided.
- Three ranges of the performances of involved heat exchangers are distinguished.
- Performance improvement results mainly from reducing the exergy destruction within the boiler.
- The fuel-savings potentials by improving each component in isolation are quantified.
- Thermodynamic interactions among components and energy-saving potentials of each component are revealed.

ARTICLE INFO

Article history:
Received 24 September 2012
Received in revised form 21 December 2012
Accepted 26 December 2012
Available online 10 February 2013

Keywords:
(Advanced) exergy analysis
Avoidable exergy destruction
Fuel-savings potential
Parametric study
Ultra-supercritical plant

ABSTRACT

In this paper, both conventional and advanced exergy analyses were conducted to a large-scale ultra-supercritical coal-fired power plant. The objectives of the conventional one are to compare the exergetic performances of different components, to identify and quantify the sites with the largest exergy destruction and losses, and to find the fuel-savings potential by improving each component in isolation. The advanced exergetic analysis focuses on the thermodynamic interactions among components and the sources for energy-saving potential of each component. Moreover, comparisons with several subcritical units are conducted and a sensitivity analysis shows the dependencies of the overall exergetic efficiency on a number of key design parameters. The results display the spatial distribution of exergy destruction and losses in detail and three performance ranges for different types of heat exchangers involved in the system. The energy-saving potentials at both the system and the component levels by improving an individual component are not in accordance with the amount of its exergy destruction. Improvement strategies for different components differ significantly due to the varied contributions of endogenous/exogenous parts to their avoidable exergy destructions. With an increase in the steam conditions, the exergy destruction ratio of the boiler is significantly reduced, contributing mainly to the system improvement. The most effective and achievable measure for reducing the fuel consumption is still the reasonable utilization of available low-grade heat. This framework provides a basis for the quantifying proposals of exergy-driven strategies for improving the system.

1. Introduction

Coal currently accounts for 29.6% of global energy consumption [1] and plays a vital role in electricity generation worldwide, contributing 41% of global electricity in 2010 [2]. The percentages of electric power derived from coal in South Africa and Poland even reach as high as 93% and 92%, respectively [2]. The power supply in the biggest electricity consumers, including China, USA and Germany, also depends highly on coal with its contributions reaching 79%, 49% and 46%, respectively [3,4]. Moreover, the importance of coal to electricity generation worldwide is set to continue, with coal fuelling approximately 44% of global electricity in 2030 according to [2].

With such a coal consumption, controlling the pollutants emissions is an unavoidable topic. To achieve sustainable development, the focus on power system efficiency moves from analysis of just economic benefits to environmental efficiency studies that assess both economic benefits and carbon emissions [5]. Thus, new technologies such as CO_2 capture have the potential to significantly reduce pollutant emissions. However, industrial tests and techno-

* Corresponding author at: School of Energy, Power and Mechanical Engineering, North China Electric Power University, Beinong Road 2, Beijing 102206, China.
E-mail address: lgwangeao@163.com (L. Wang).

0306-2619/$ - see front matter © 2013 Elsevier Ltd. All rights reserved.
http://dx.doi.org/10.1016/j.apenergy.2012.12.063

Nomenclature

APH	air preheater
AT	spray attemperator
BP	the basic or real plant
CAV	cavity
CC	combustion process (chamber)
COND	condenser
CP	coal-fired power
CDP	condensate pump
DA	deaerator
ECON	economizer
FC	fuel consumption
FP	feedwater pump
FRH	final reheater
FSH	final superheater
G	electric generator
H*n*	the *n*th feedwater preheater
HHV	higher heating value
HPRH	horizontal primary reheater
HPT	high pressure turbine
IPT	intermediate pressure turbine
LF	lower part of the furnace
LHV	lower heating value
LPT	low pressure turbine
PP	percentage point
PR	pendant-tube riser
PSH	platen-type superheater
RAH	reversible adiabatic heater
SSH	screen-type superheater
ST	the secondary turbine
SUB	sub-critical
UF	upper part of the furnace
USC	ultra-supercritical
VPRH	vertical primary reheater
WSPSH	component with waterwall, SSH and PSH

Greek symbols

α	air–fuel ratio
Δ	difference
ε	exergy efficiency

Mathematical symbols

$\dot{E}_D$	exergy destruction
$\dot{E}_F$	fuel exergy
$\dot{E}_L$	exergy loss
$\dot{E}_P$	product exergy
$\dot{m}$	mass flow rate
$\dot{Q}$	heat
η_m	mechanical efficiency
η_s	isentropic efficiency
$\triangle \dot{E}^{*,k}_{F,tot}$	the energy-saving limit of FC by improving the *k*th component
P	power output
p	pressure
t,T	temperature
y_D	exergy destruction ratio

Superscripts

AV	avoidable
EN	endogenous
EX	exogenous
UN	unavoidable
R	the real cycle or conditions
T	the theoretical cycle or conditions

Subscripts

a	average
c, *h*	cold or hot stream
ex	exhaust
fg	flue gas
fw	feedwater
i,*o*	incoming or outgoing stream
ms,*sh*	main steam or superheated steam
pinch	pinch point
rh	reheated steam
k	the *k*th component
tot	the overall system

economic analysis of CO_2 capture in a demonstrating coal-fired power station [6] show that the electricity purchase price increases by 29% with CO_2 capture. In fact, currently new technologies (not only CO_2 capture and sequestration) for reducing pollution from power generation are regarded too risky or too expensive [7]. Thus, the best alternative for reducing emissions is still to increase the plant efficiency.

In this context, supercritical and ultra-supercritical (USC) coal-fired power (CP) generation is regarded to be significant [8]. The technology currently achieves a plant efficiency of 45% (LHV basis) with the main steam parameters limited at about 300 bar and 600 °C [9]. In China, over 50 USC CP power generation units using these steam conditions with a capacity of 1000 MW have been under construction or put into operation. Higher parameter USC cycles aiming at a temperature of 700 °C (or even 760 °C) and higher pressures in the near future promise to generate electricity at a higher efficiency, approaching 50% (LHV) [10–15], with proper approaches for reducing gross heat losses, for example, reducing unburned combustible loss [16,17] and advanced waste heat-water recovery technology [18]. Following Europe, Japan and USA, China also announced the research and development of USC CP plants aiming at steam conditions of 36.65 Mpa/705 °C/723 °C/723 °C. Thus, thethermodynamic performance of power plants with such high parameters needs to be detailed evaluated for deep insights of component behaviors and for finding more promising improvement approaches.

The exergy analysis of thermal power plant began from 1970s. In 1980s, Moran [19,20], Kostas [21] and Szargut et al. [22] discussed the exergy analysis of thermal systems. Later, Bejan et al. [23], and Lazzaretto and Tsatsaronis [24] contributed to the exergy-based analysis and its application to various systems. In the last decade, this method has been widely applied to a wide range of thermal power plants. Tsatsaronis [25] performed an exergetic analysis to a complex steam power plant and identified the potentials for further improvement. Horlock et al. [26] also conducted exergy analyses of fossil-fuel power plants and discussed the differences among three derived efficiencies. Dincer and Al-Muslim [27] analyzed reheat-cycle steam power plants by using exergy analysis. Sengupata et al. [28] applied exergy analysis to a coal-based 210 MW thermal power plant using design parameters and discussed its exergetic performances under different loads. Similarly, Aljundi [29] conducted energy and exergy analysis to a 396 MW power plant and proposed an estimation of plant performance. Wang et al. [30] performed exergy analysis to compare the performance of differential waste heat recovery approaches and arrangements for a cement cogeneration power plant. Moreover,

Ray et al. [31] conducted exergy analysis to a 500 MW steam turbine cycle under design and off-design conditions and attempted to identify the contribution of individual equipment in the overall increase of exergy destruction under off-design condition. Additionally, Suresh et al. [32] carried out a thermodynamic analysis based on exergy to compare the performances of optimal solutions from different optimization methods. However, the aforementioned conventional analyses can only provide a rough distribution of exergy destruction and losses within the energy systems but cannot quantify the energy-saving potential of an individual component and the thermodynamic interactions among different components.

Therefore, recent developments [33–39] of exergy analysis, including the advanced exergy analysis, concentrate on the revelation of the sources and the potential of reduction of exergy destruction. Thereafter, the advanced exergy analysis has been successfully applied to a simple open gas-turbine system [40], a simple vapor-compression refrigeration machine [41], a novel cogeneration system for vaporizing liquefied natural gas [42], a three-pressure level combined cycle [42] and a steam methane reforming system for hydrogen production [43]. It has been proven that the advanced analysis is a promising and powerful tool for comprehensively evaluating complex energy systems. Thus, Wang et al. [44] applied an advanced exergy analysis to a simplified CP plant for novel improvement strategies; however, the boiler was taken as a black box, leading to lack of knowledge on the interactions among the components in the boiler subsystem.

This paper focuses on the deep and complete discussion of the exergetic performance of an existing USC CP plant with a total capacity of 660 MW and 1913 t/h main steam. To our best knowledge, it would be the first article which provides such comprehensive information of a state-of-the-art USC CP plant on the basis of the second law of thermodynamics. In this regard, the specific objectives of this paper are (1) to conduct a conventional exergy analysis for the complete spatial distribution of exergy destruction and losses, (2) to deeply discuss the exergetic performance of different types of heat exchangers, (3) to quantitatively calculate the energy-savings potential of the overall system when improving one component in isolation, (4) to perform an advanced exergy analysis for revealing component interactions and the true potential for reducing the exergy destruction within each component, (5) to present the sensitivities of the overall exergetic efficiency on various key design variables of the power plant, and (6) to compare the thermodynamic behaviors at both the component and system levels with three existing subcritical plants with different capacities and to find novel and promising approaches for improving future plant designs.

2. Methodology

2.1. Exergy analysis

The exergy analysis identifies the location, the magnitude and the sources of thermodynamic inefficiencies in a thermal system [23,45]. The following variables [23,45,46] are generally used for the exergetic evaluation of an individual component and the overall system: exergy destruction rate within the kth productive component

$$\dot{E}_{D,k} = \dot{E}_{F,k} - \dot{E}_{P,k}, \tag{1}$$

the exergetic efficiency of the kth productive component

$$\varepsilon_k = \dot{E}_{P,k}/\dot{E}_{F,k} = 1 - \dot{E}_{D,k}/\dot{E}_{F,k}, \tag{2}$$

and the exergy destruction ratio of the kth component

$$y_{D,k} = \dot{E}_{D,k}/\dot{E}_{F,tot}. \tag{3}$$

The exergy balance of the overall system can be written as

$$\dot{E}_{F,tot} = \dot{E}_{P,tot} + \sum \dot{E}_{D,k} + \dot{E}_{L,tot}. \tag{4}$$

The handling of exergy losses and dissipative components, such as condenser, gas cleaning units and throttle valves, can be found in [24,45].

Detailed calculation methods for physical and chemical exergies of different types of material flows, work and heat flows are discussed in [20,23,45]; however, it should be noted here that the chemical exergy of coal is calculated by multiplying its *HHV* with a constant factor, normally 1.02 [23,47]. In addition, the reference environment for chemical exergy is taken as the model developed by Ahrendts [48] with the reference temperature and pressure 298.15 K and 1 bar, respectively.

2.2. Fuel-savings potential by improving an individual component

Due to the relative location of one component to the final product, the contributions of the same irreversibilities occurring in different components to the fuel consumption (FC) varies significantly.

Considering the thermodynamic limits, the best possible condition of one components can be regarded as the so-called theoretical condition. Accordingly, the energy-savings potential by improving an individual component $\left(\triangle E^{*,k}_{F,tot}\right)$ can be primarily calculated as the following equation:

$$\triangle E^{*,k}_{F,tot} = E^{R}_{F,tot} - E^{T,k}_{F,tot} \tag{5}$$

where $E^{R}_{F,tot}$ indicates the fuel exergy consumption of the overall system when all components are under their real processes, while $E^{T,k}_{F,tot}$ represents that of the hybrid process (*hybrid I*) of the kth component, in which only the considered component operates theoretically while all the remaining components perform with their real processes.

The theoretical conditions for different components should follow the assumptions: $\dot{E}_D = 0$ (if possible) or otherwise $\dot{E}_D = min$. For turbo-machinery including turbine, fan and pump, the isentropic efficiency (η_s) and mechanical efficiency (η_m) should be unity. With respect to an individual heat exchanger, both pressure drops ($\triangle p$) and pinch temperature difference ($\triangle T_{pinch}$) should equal zero. Detailed descriptions on the theoretical conditions of combustion chamber can be found in [36].

2.3. Advanced exergy analysis

The thermodynamic behavior of one component is largely related to the properties of its connected streams and, thus, interactions among different components may be of great importance. Moreover, due to technical and economic limitations and manufacturing methods, each component has an unapproachable best thermodynamic behavior in the near future that determines its true energy-saving potential. Therefore, advanced exergy analysis was applied to reveal the sources (endogenous/exogenous) and the potential for reduction (avoidable/unavoidable) of exergy destruction.

2.3.1. Endogenous/exogenous exergy destruction

The endogenous part is the exergy destruction obtained when all other components operate theoretically and the component being considered operates with its real condition. While the exogenous part of the exergy destruction within the considered component, is caused by irreversibilities in the remaining components and by the structure of the overall system, and is the difference between total exergy destruction of the component at real conditions

and the endogenous part [41]. In this way, the exergy destruction within the kth component can be readily split as Eq. (6).

$$\dot{E}_{D,k} = \dot{E}^{EN}_{D,k} + \dot{E}^{EX}_{D,k} \tag{6}$$

2.3.2. Avoidable/unavoidable exergy destruction

The unavoidable part is the part that cannot be eliminated, even if the best available technology in the near future would be applied, and, correspondingly, the avoidable part is the difference between the total exergy destruction within the component in the real plant and the unavoidable part of exergy destruction [41]. When all components operate with their best possible conditions, the unavoidable process is established to obtain the ratios $(\dot{E}_D/\dot{E}_P)^{UN}_k$. Thereafter, $\dot{E}^{UN}_{D,k}$ of each component can be readily calculated by

$$\dot{E}^{UN}_{D,k} = \dot{E}_{P,k} \cdot (\dot{E}_D/\dot{E}_P)^{UN}_k \tag{7}$$

Then, the exergy destruction within the kth component can also be written as:

$$\dot{E}_{D,k} = \dot{E}^{AV}_{D,k} + \dot{E}^{UN}_{D,k} \tag{8}$$

2.3.3. Combination of the splitting

By further combining the two splitting concepts, the avoidable-endogenous $\left(\dot{E}^{AV,EN}_{D,k}\right)$/avoidable-exogenous $\left(\dot{E}^{AV,EX}_{D,k}\right)$ and unavoidable-endogenous $\left(\dot{E}^{UN,EN}_{D,k}\right)$/unavoidable-exogenous $\left(\dot{E}^{UN,EX}_{D,k}\right)$ terms can be obtained from:

$$\dot{E}^{UN,EN}_{D,k} = \dot{E}^{EN}_{P,k} \cdot (\dot{E}_D/\dot{E}_P)^{UN}_k \tag{9a}$$

$$\dot{E}^{UN,EX}_{D,k} = \dot{E}^{UN}_{D,k} - \dot{E}^{UN,EN}_{D,k} \tag{9b}$$

$$\dot{E}^{AV,EN}_{D,k} = \dot{E}^{EN}_{D,k} - \dot{E}^{UN,EN}_{D,k} \tag{9c}$$

$$\dot{E}^{AV,EX}_{D,k} = \dot{E}^{EX}_{D,k} - \dot{E}^{UN,EX}_{D,k} \tag{9d}$$

The calculation of the aforementioned four parts starts from the determination of the ratio $(\dot{E}_D/\dot{E}_P)^{UN}_k$, $\dot{E}^{EN}_{D,k}$ and $\dot{E}^{EN}_{P,k}$, with the assistances of unavoidable and *hybrid II* processes. In a *hybrid II* process, only the component being considered is set to its real condition while the remaining components operate with their theoretical conditions. Additionally, the theoretical conditions mentioned here are treated the same as in Section 2.2.

3. Plant description

The USC CP plant, with the main design parameters listed in Table 1 and the flow sheet shown in Fig. 1, has a total installed capacity of 660 MW, consisting of a boiler subsystem and a turbine subsystem. The bituminous coal with *LHV* (21981 kJ/kg) and the ultimate analysis (as received basis) of C (57.52%), H (3.11%), O (2.78%), N (0.99%), S (2.00%) and H_2O (9.9%) is considered as the fuel.

By modeling the boiler subsystem into 12 sections (I–XII), detailed calculations of heat transfer were conducted to simulate its performance as precise as possible for conventional exergy analysis. Each involved section consists of a flue duct, a main heating surface (as shown in Fig. 1) and auxiliary heating surfaces (if exists). The feedwater from the regeneration subsystem flows through ECON and water walls of sections I–VI with phase transition. Then, the generated steam passes through various auxiliary heating surfaces, including the roof tubes and sidewall tubes corresponding to each main heating surface. Thereafter, the main steam flows to HPT after further heated to 571 °C in SSH, PSH and FSH. To regulate the steam temperature, two stage attemperators (AT1 and AT2) are configured before and after PSH.

The main steam expands through stages of HPT, IPT and LPT to generate the shaft work for electricity. Then, the final exhausted steam is condensed in a surface COND. To increase the thermal efficiency of the steam cycle, parts of the expanded steam is extracted at different locations of the turbine to heat the feedwater in regeneration subsystem, including four low-pressure ones (H5–H8), one deaerator (DA) and three high-pressure ones (H1–H3). In addition, one ST, which uses the same steam extraction as DA, is configured to meet the large amount of power required by FP.

The thermodynamic properties of the streams involved in the real conditions of both the boiler and turbine subsystems are listed in Tables A.1 and A.2, respectively.

Table 1
Key design parameters of the USC power generation unit.

Name	Value	Name	Value
$\dot{m}_{ms}$	1913 t/h	$p_{rh,h}$	42 bar
t_{ms}	571 °C	$\dot{m}_{coal}$	250.74 t/h
p_{ms}	254 bar	t_{fw}	282 °C
$\dot{m}_{rh}$	1584 t/h	p_{fw}	293.5 bar
$t_{rh,c}$	312 °C	p_{COND}	5.88 kPa
$p_{rh,c}$	43.9 bar	$t_{ex,fg}$	127 °C
$t_{rh,h}$	569 °C	P_{tot}	670 MW

4. Real, theoretical and unavoidable conditions

In accordance with Sections 2.2 and 3, the assumptions of the theoretical, real and unavoidable conditions for different components in the system are listed in Table 2. With regards to the unavoidable conditions, it would be better if the best performance characteristics can be derived in conjunction with some kind of investment-efficiency considerations or the best practice of the same type components under operation; otherwise, the best behavior is determined more or less arbitrarily, depending highly on the understanding and practical experience of the analyzer.

The assumptions of the components in the boiler subsystem are rather tricky, since the theoretical operation of a concurrent heater may defect its succeeding heaters due to the facts that the temperature of the steam out of the heater working theoretically may exceed the allowed temperature of its following component, such as turbine, or the temperature of the flue gas entering its successive heater may be below the corresponding steam temperature. Thus, as is shown in Fig. 2, one reversible adiabatic heater (RAH), the approach described in [38,41,43], is added before each heater exchanger and the target of each heater is set to heat the working fluid to a specified temperature. The RAHs are off under real processes but can be active by separating the temperatures (enthalpies) of its connected flue gases. In this way, the calculation of one heat exchanger starts from computing the heat absorbed by the steam and then the temperature of the flue gas entering the heater can be obtained with the pre-calculated mass flow rate of the flue gas from the heat balance of the boiler subsystem. It should also be mentioned here, for simplicity, the combustion process (CC) is considered as one separate component, and the water wall, SSH and PSH are also regarded to be one component (WSPSH) because these three concurrent heaters are arranged sequentially along the flue gas.

In addition, the simulations for fuel-savings potentials and advanced exergy analysis are conducted with the help of a professional simulator, Ebsilon Professional [49].

5. Results and discussion

5.1. Exergetic performance analysis

The results of conventional exergy analysis at the component level are presented in Table 3.

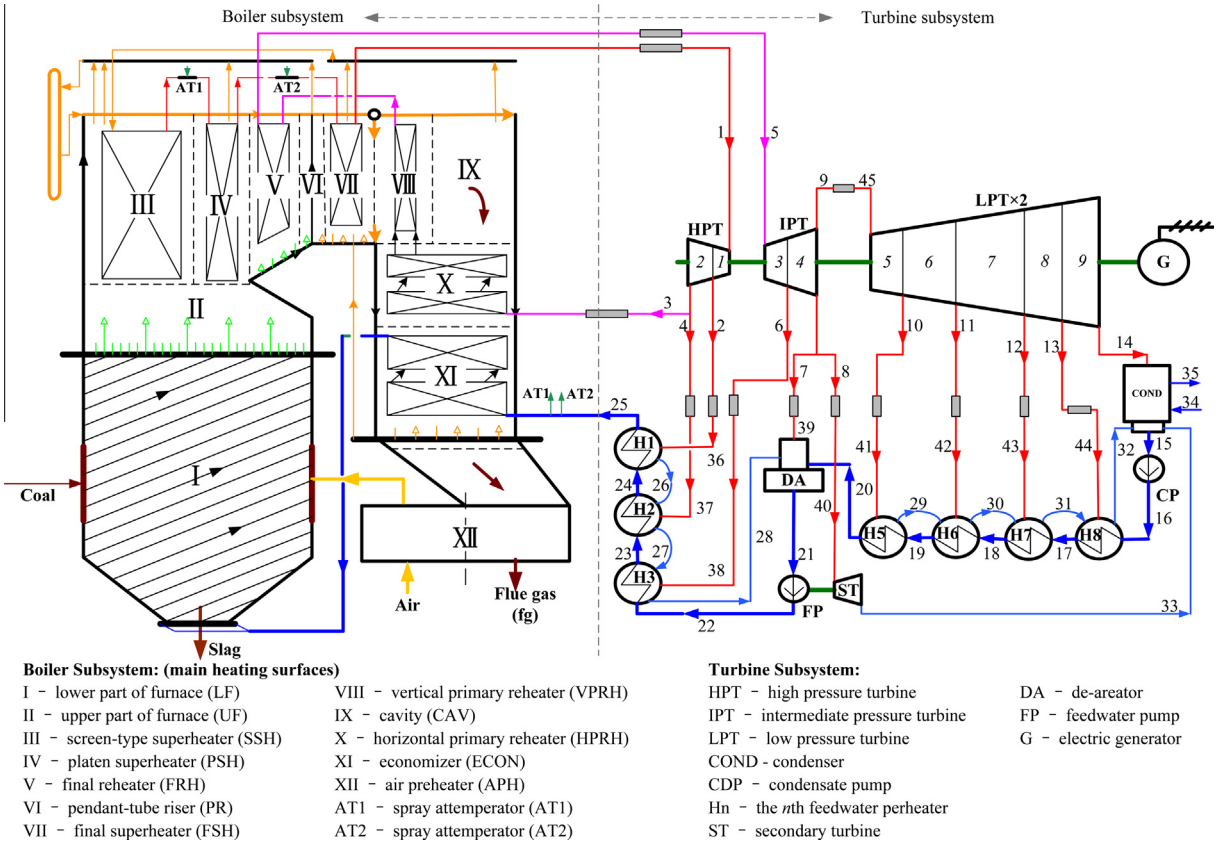

Fig. 1. Schematic diagram of the overall USC power generation unit.

Table 2
Real, theoretical and unavoidable conditions of different components (t – °C; p – bar).

Comp.	REAL	TH	UN	Comp.	REAL	TH	UN
CC[a]	$\alpha = 1.15$	$\alpha = 1.15$	$\alpha = 1.03$	H8	$\triangle t_{pinch} = 2.8$	$\triangle t_{pinch} = 0$	$\triangle t_{pinch} = 1.5$
	$\eta_c = 0.987$	$\eta_c = 1$	$\eta_c = 1$		$\triangle p_{fw} = 1.4$	$\triangle p_{fw} = 0$	$\triangle p_{fw} = 0.5$
WSPSH	$\triangle p_{wf} = 32.7$	$\triangle p_{wf} = 0$	$\triangle p_{wf} = 15.0$	H7	$\triangle t_{pinch} = 2.8$	$\triangle t_{pinch} = 0$	$\triangle t_{pinch} = 1.5$
	$\triangle t_{pinch} = 536$	$\triangle t_{pinch} = 0$	$\triangle t_{pinch} = 100$		$\triangle p_{fw} = 1.3$	$\triangle p_{fw} = 0$	$\triangle p_{fw} = 0.6$
FRH	$\triangle p_{wf} = 0.9$	$\triangle p_{wf} = 0$	$\triangle p_{wf} = 0.5$	H6	$\triangle t_{pinch} = 3.13$	$\triangle t_{pinch} = 0$	$\triangle t_{pinch} = 1.67$
	$\triangle t_{pinch} = 373$	$\triangle t_{pinch} = 0$	$\triangle t_{pinch} = 100$		$\triangle p_{fw} = 1.6$	$\triangle p_{fw} = 0$	$\triangle p_{fw} = 0.5$
FSH	$\triangle p_{wf} = 4$	$\triangle p_{wf} = 0$	$\triangle p_{wf} = 2.0$	H5	$\triangle t_{pinch} = 6.31$	$\triangle t_{pinch} = 0$	$\triangle t_{pinch} = 4.24$
	$\triangle t_{pinch} = 249$	$\triangle t_{pinch} = 0$	$\triangle t_{pinch} = 100$		$\triangle p_{fw} = 1.5$	$\triangle p_{fw} = 0$	$\triangle p_{fw} = 0.7$
PRH	$\triangle p_{wf} = 1$	$\triangle p_{wf} = 0$	$\triangle p_{wf} = 0.5$	H3	$\triangle t_{pinch} = 5.27$	$\triangle t_{pinch} = 0$	$\triangle t_{pinch} = 4.27$
	$\triangle t_{pinch} = 272$	$\triangle t_{pinch} = 0$	$\triangle t_{pinch} = 100$		$\triangle p_{fw} = 5.0$	$\triangle p_{fw} = 0$	$\triangle p_{fw} = 2.4$
ECON	$\triangle p_{wf} = 2$	$\triangle p_{wf} = 0$	$\triangle p_{wf} = 1.0$	H2	$\triangle t_{pinch} = 3.02$	$\triangle t_{pinch} = 0$	$\triangle t_{pinch} = 1.40$
	$\triangle t_{pinch} = 102$	$\triangle t_{pinch} = 0$	$\triangle t_{pinch} = 50$		$\triangle p_{fw} = 5.3$	$\triangle p_{fw} = 0$	$\triangle p_{fw} = 2.5$
APH[b]	$\triangle p_{air} = 0$	$\triangle p_{air} = 0$	$\triangle p_{air} = 0$	H1	$\triangle t_{pinch} = 2.7$	$\triangle t_{pinch} = 0$	$\triangle t_{pinch} = 1.82$
	$\triangle t_{pinch} = 102$	$\triangle t_{pinch} = 0.0$	$\triangle t_{pinch} = 65$		$\triangle p_{fw} = 5.5$	$\triangle p_{fw} = 0$	$\triangle p_{fw} = 2.7$
HPT1[c]	$\eta_s = 0.888$	$\eta_s = 1.0$	$\eta_s = 0.900$	LPT5	$\eta_s = 0.820$	$\eta_s = 1.0$	$\eta_s = 0.850$
HPT2	$\eta_s = 0.880$	$\eta_s = 1.0$	$\eta_s = 0.920$	COND	$\triangle t_{pinch} = 5.0$	$\triangle t_{pinch} = 0$	$\triangle t_{pinch} = 3.0$
IPT1	$\eta_s = 0.918$	$\eta_s = 1.0$	$\eta_s = 0.960$	CDP	$\eta_s = 0.803$	$\eta_s = 1.0$	$\eta_s = 0.870$
IPT2	$\eta_s = 0.930$	$\eta_s = 1.0$	$\eta_s = 0.960$	DA	$\Delta p = 1.0$	$\Delta p = 0.0$	$\Delta p = 0.3$
LPT1	$\eta_s = 0.939$	$\eta_s = 1.0$	$\eta_s = 0.960$	FP	$\eta_s = 0.840$	$\eta_s = 1.0$	$\eta_s = 0.910$
LPT2	$\eta_s = 0.965$	$\eta_s = 1.0$	$\eta_s = 0.980$	ST	$\eta_s = 0.800$	$\eta_s = 1.0$	$\eta_s = 0.880$
LPT3	$\eta_s = 0.922$	$\eta_s = 1.0$	$\eta_s = 0.940$	G	$\eta_m = 0.985$	$\eta_m = 1.0$	$\eta_m = 0.993$
LPT4	$\eta_s = 0.738$	$\eta_s = 1.0$	$\eta_s = 0.850$				

[a] $\triangle p$ of flue gas and air is neglected for real, theoretical and unavoidable conditions.
[b] $\triangle t_{pinch}$ for real and unavoidable conditions is taken as the lower terminal temperature difference, while that of the theoretical condition is the upper one.
[c] η_s of the turbo-machinery is 0.998, 1.0 and 0.999 for real, theoretical and unavoidable conditions, respectively.

5.1.1. The boiler subsystem

It can be seen from Table 3 that the Section I, where the fierce chemical reaction occurs, dominates the total irreversibility in boiler subsystem with its exergetic efficiency as low as 67%. It indicates that one third of total input of fuel exergy is destructed.

Table 3 also shows that the thermodynamic inefficiencies of heating surfaces in Sections I–IV, in which the radiation heat transfer is prevailing, are generally larger than those of convection heating surfaces in the following flue gas duct. The reason for this can be clearly explained by Fig. 3. The radiation heat transfer can be the

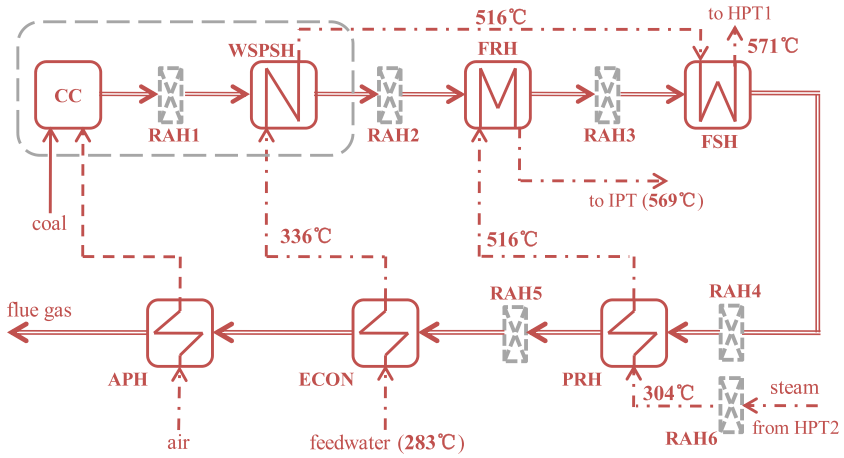

Fig. 2. Simplified flow diagram of boiler subsystem for advanced exergy analysis.

Table 3
Results of the conventional exergy analysis at the component level.

Comp.	$\dot{E}_{F,k}$ (MW)	$\dot{E}_{P,k}$ (MW)	$\dot{E}_{D,k}$ (MW)	$y_{D,k}$ (%)	ε_k (%)
LF	1652	1112	539	33.3	67.5
UF	117	82.9	34.0	2.10	70.9
SSH	118	85.1	33.4	2.06	71.8
PSH	91.3	69.5	21.8	1.34	76.2
FRH	74.8	58.2	16.6	1.02	77.8
PR	12.0	8.78	3.20	0.20	73.3
FSH	95.2	78.6	16.6	1.02	82.6
VPRH	24.6	19.5	5.07	0.31	79.4
CAV	11.3	8.90	2.37	0.15	79.0
HPRH	111	87.6	23.8	1.47	78.6
ECON	85.6	69.3	16.3	1.00	81.0
APH	78.7	57.4	21.3	1.31	73.0
HPT1	184	173	10.6	0.67	94.2
HPT2	46.2	43.1	3.09	0.19	93.3
IPT1	104	99.9	3.88	0.24	96.3
IPT2	83.5	80.5	3.02	0.19	96.4
LPT1	83.1	80.0	3.12	0.20	96.2
LPT2	85.8	83.3	2.43	0.15	97.2
LPT3	40.0	37.3	2.68	0.17	93.3
LPT4	53.9	40.8	13.0	0.82	75.8
LPT5	52.2	43.0	9.22	0.58	82.4
COND	24.7	–	24.7	1.52	–
CDP	0.87	0.70	0.17	0.01	80.7
H8	3.58	2.38	1.20	0.08	66.3
H7	7.67	6.03	1.64	0.10	78.6
H6	7.04	6.18	0.86	0.05	87.8
H5	19.3	16.3	3.00	0.19	84.4
DA	24.0	20.7	3.33	0.21	86.1
FP	20.1	18.0	2.09	0.13	89.6
H3	25.1	22.7	2.39	0.15	90.5
H2	46.4	43.8	2.58	0.16	94.4
H1	32.0	30.9	1.12	0.07	96.5
ST	24.8	20.1	4.75	0.30	80.9
G	681	671	9.53	0.60	98.6
Total	1621	670	843	52.0	41.4

leading heat transfer mode only when the flue gas temperature is extremely high, causing the high temperature difference between flue gas and working fluid at the mean time. This especially happens to the water wall in Section I, that encloses the flue gas with highest spot temperature and flows the working fluid with almost the lowest temperature. While in the convection-leading heating surface, the heat release from hot side to cold side is far less fierce than that of radiation and the temperature difference of heat transfer is also much less. As a consequence, relatively higher exergetic efficiencies are achieved in the sections of the post flue duct.

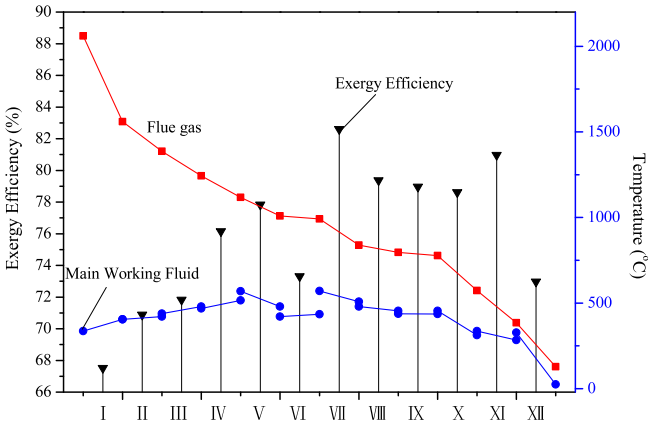

Fig. 3. Temperature profiles of fluids and exergy efficiency of different sections in boiler subsystem.

It should be mentioned here that the calculated exergy efficiency of air preheater is obviously lower than that of other convection heat surfaces though the air heating is under lowest temperature difference. This is the result of low temperature level of heat transfer, which increases the thermodynamic irreversibility.

5.1.2. The turbine subsystem

The turbine stages working in the range of superheated steam show great performance with little thermodynamic inefficiencies and their exegetic efficiencies reaching 93–97%, while the ones driven by wet steam tend to have worse working conditions with the efficiencies sharply decreasing to 75–82%. This is mainly due to the wetness loss and the tip clearance loss as well as to enormously increased residual speed loss of the last turbine stage.

In general, the exergetic performances of regenerative preheaters improve steadily along the flow direction of feedwater as shown in Fig. 4. This is because the higher the temperature level of the cold fluid, the greater the exergy efficiency, for heat transfer processes having the same temperature difference. However, deviations of H5, H3 and H2 from the main trend should also be highlighted. Large temperature difference of the condensate section is the main reason for the deviation of H5 and H2, while that of H3 is due to the high temperature steam extraction after reheat.

5.1.3. Further discussion on exergetic performances of heat exchangers

As mentioned above, the temperature level of the cold fluid and the temperature difference for heat transfer are generally regarded

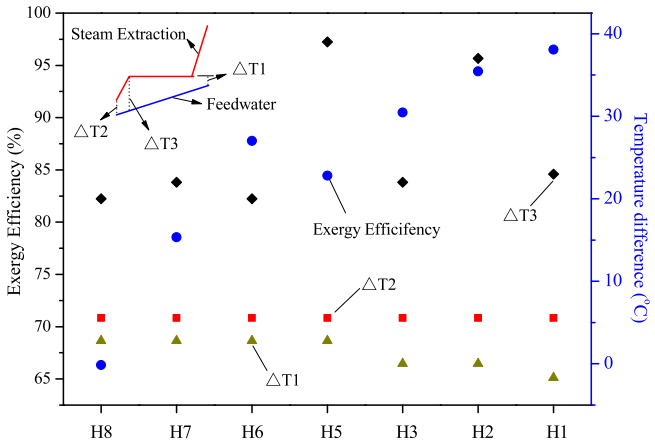

Fig. 4. Exergy efficiencies and temperature differences of all closed-type preheaters.

as two key factors characterizing the exergetic performances of different heaters. However, how and to what extend do these factors determine the exergy efficiency have never been discussed before.

In accordance with Eq. (2), the exergy efficiency of a productive heat exchanger can be generally written as follows

$$\varepsilon = \frac{E_{o,c} - E_{i,c}}{E_{i,h} - E_{o,h}} = \frac{\dot{Q}(1 - T_0/T_{a,c})}{\dot{Q}(1 - T_0/T_{a,h})} \tag{10}$$

where $T_{a,h}$ and $T_{a,c}$ represent the thermodynamic average temperatures of hot stream and cold stream, respectively.

Substituting $T_{a,h}$ by $T_{a,c} + \Delta T$, Eq. (10) can be rewritten as

$$\varepsilon = \frac{1 - T_0/T_{a,c}}{1 - T_0/(T_{a,h} + \Delta T)} \tag{11}$$

Therefore, the dependencies of exergy efficiency with $T_{a,c}$ (three temperature ranges A, B and C) and ΔT (different values corresponding to range A, B and C) can be shown in Fig. 5. It is apparent that, for a constant temperature difference, the higher the average temperature of the cold fluid, the larger the exergy efficiency of the heat exchanger.

Range A stands for the working region of feedwater preheaters with $T_{a,c}$ (35–250 °C) and ΔT (0.5–5 °C). It is quite clear that the exergy efficiency increases sharply with the increase of both $T_{a,c}$ and ΔT when $T_{a,c}$ is lower than 70 °C. Thereafter, ΔT becomes the dominating factor while the influence of $T_{a,c}$ tends to be weak. In addition, when $T_{a,c}$ is larger than 200 °C, the exergy efficiencies of the preheaters will be higher than 95% indicating very good performance. However, due to the lowest $T_{a,c}$ in H8, its exergy efficiency is only 66% as that of Section I in the boiler subsystem.

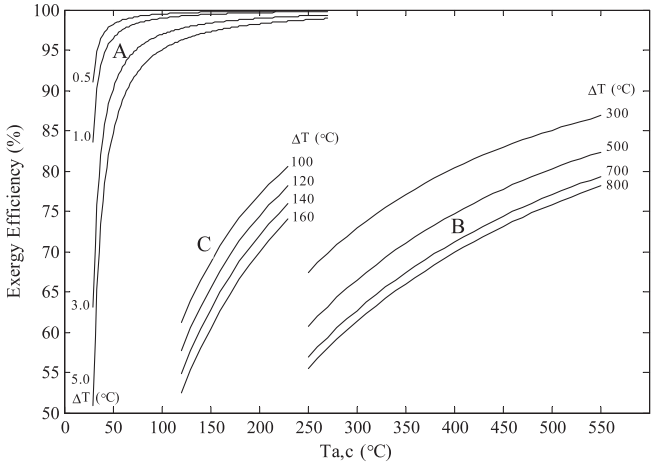

Fig. 5. Exergy efficiency vs. temperature level and difference of heat exchangers.

Range B represents the working zone of heating surfaces in the boiler subsystem. The exergy efficiencies of radiation-dominated heating surfaces are usually lower than 80%. Because the flue gas temperature decreases dramatically in radiation sections, the convection heat sections always have relatively high efficiency. However, the performances of these heat surfaces tend to have small fluctuations due to the variation of inlet temperature of cold fluid caused by the complex arrangement of water and steam pipelines in boiler subsystem.

Range C denotes the working region of air preheater whose inlet temperature of cold fluid is always as low as the environment temperature. It can be seen that the exergetic efficiency of air preheaters generally falls within the range from 70% to 80% and is lower than those of convection heating surfaces.

5.2. Distribution of exergy destruction and losses

It can be seen from Fig. 6a that the exergy destruction within the boiler subsystem (77%) dominates the overall exergy dissipation, followed by that within the turbine subsystem (over 11%) and the total exergy loss (over 9%). Thus, the boiler subsystem may be where the largest energy-savings potential may exist.

Fig. 6b demonstrates the spatial distribution of exergy losses of the whole system. The boiler exhaust (75%) contributes the largest proportion of exergy losses and the boiler slag (15%), system cold end (7%) and boiler surface (3%) have much lower contributions. Apparently, the efficient utilization of the large amount of exergy of waste flue gas should be further investigated for the further reduction of FC.

Fig. 6c shows that the largest proportion (over 73%) of exergy destruction within the boiler subsystem comes from Section I, while the destructions within other sections are much smaller. It is, therefore, indicated that much more attention should be paid to the improvement of exergy transportation process from the fuel exergy to the physical exergy of steam.

Fig. 6d illustrates that the exergy destruction within the turbine subsystem is dominated by the turbine itself (almost 50%), followed by the condenser (18%), while the feedwater preheating subsystem contributes only a little bit more than 12%. This emphasizes the significance of advanced design of turbine blades, particularly the blades working in wet steam range, and also the topology optimization of feedwater preheating subsystem. It should be noted that although high efficiency is achieved in various pipelines, the accumulated exergy destruction is still very large and contributes over 10% to the exergy destruction within the turbine subsystem.

5.3. Comparison with existing sub-critical plants

Comparisons with three different existing sub-critical plants with parameters shown in Table 4 are conducted to illustrate whether only exergy destructions within certain components of the USC plants are significantly reduced or all the exergy destructions are homogeneously lowered. Fig. 7 and Table 4 clearly present that with the increase of steam conditions and the final feedwater temperature, the exergy destruction ratio of the boiler reduces significantly followed by the turbines, which mainly contribute to the improvement of the overall exergy efficiency, while the ratios of condenser, feedwater regeneration subsystem and others remain almost the same. Meanwhile, the ratio of total exergy losses to the overall fuel exergy also keeps nearly unchanged with existing designs.

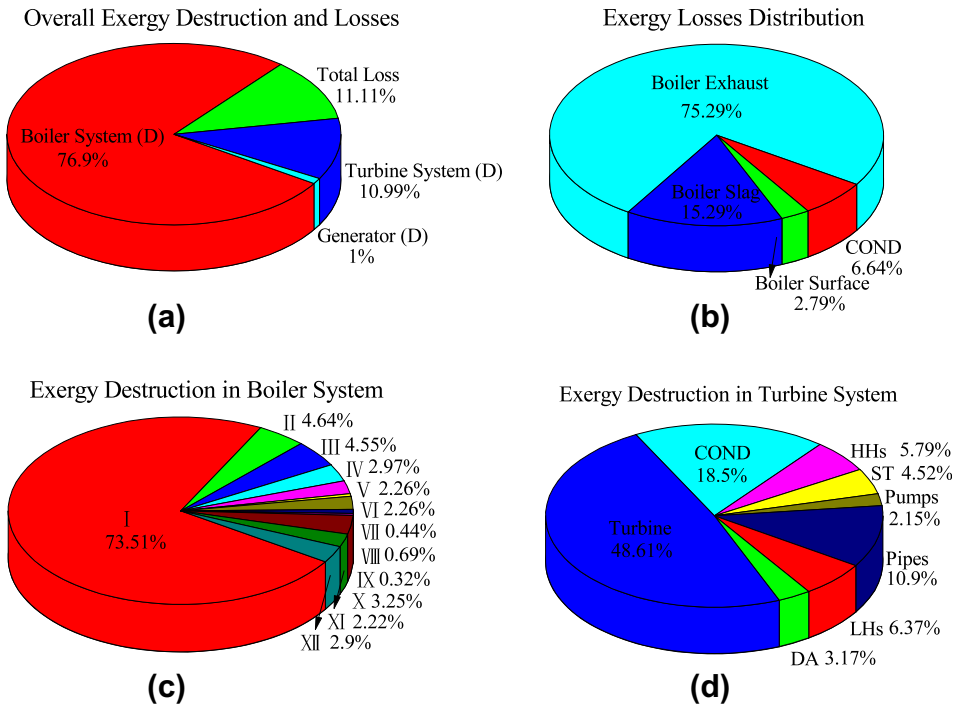

Fig. 6. Spatial distribution of exergy dissipation (destruction and losses).

Table 4
Key design parameters of three selected existing subcritical (SUB) plants in China.

Size (MW)	$\dot{m}_{ms}$ (t/h)	$p_{ms}/t_{ms}/p_{rh,h}/t_{rh,h}$ (bar/°C/bar/°C)	p_{fw}/t_{fw} (bar/°C)	p_{COND} (kPa)
220 [50]	670	137/541/24.7/541	158/240	5.20
330 [51]	938	175/541/36.4/541	192/281	4.90
660 [52]	2026	175/541/36.4/541	192/279	5.88

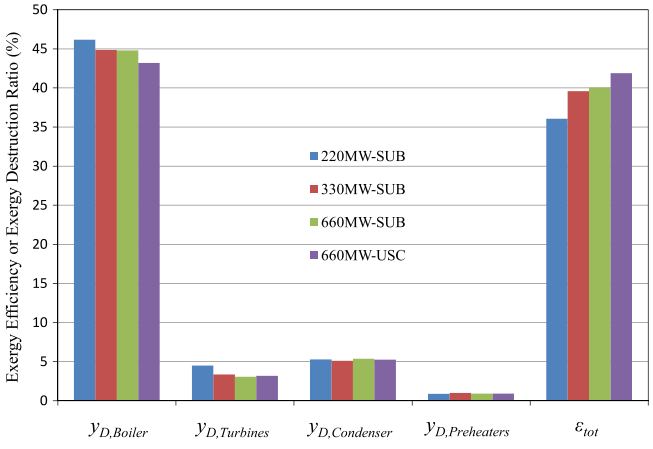

Fig. 7. Comparisons with various sub-critical plants.

5.4. Discussion on fuel-savings potential

The fuel-savings potential of the overall system when improving each component in isolation are listed in Table 5. Provided the existing conversion mode from the fuel exergy to the flue gas exergy, the arrangements of heating surfaces and the specified power output, the total fuel-savings potential by improving components in the boiler subsystem is far less than that of the turbine subsystem. The facts are the amounts of the main and reheat steam are absolutely determined by the turbine subsystem and, thus, the heat absorbed in the boiler is fixed, given also its conditions. This means if α and $t_{ex,fg}$ are kept constant, there will be only a limited potential to reduce FC from the boiler subsystem. In this case, only by lessening pressure drops of working fluid can FC be reduced.

Table 5 also presents that great benefits (a reduction of FC by 64 MW) can be obtained from the theoretical operations of APH and CC. Thus, the promising approaches for FC reduction from the design perspective of the boiler subsystem would be only reducing α and $t_{ex,fg}$.

With respect to the turbine subsystem, the improvements of turbo-machines, including the turbine itself, FP, ST and G, are of great importance for reducing FC, although their exergy destructions under real processes are much smaller than those of the boiler subsystem. The benefits obtained from the turbine subsystem are almost as twice as that of the boiler subsystem. In addition, the performance of an individual feedwater preheater almost has no influence on FC in this case, since the pressures of steam extractions remain unchanged for all processes.

5.5. Advanced exergy analysis

Table 5 shows that a large part of the exergy destruction within all components is endogenous. However, for different types of components, the proportions of the exogenous part differ signifi-

Table 5
Results of fuel-savings potential when isolately improving one component and advanced exergy analysis at the component level [a](unit: MW).

Comp.	$\dot{E}^{T,k}_{F,tot}$	$\dot{E}^{T}_{D,k}$	$\triangle\dot{E}^{*,k}_{F,tot}$	$\dot{E}^{R}_{D,k}$	$\dot{E}^{EN}_{D,k}$	$\dot{E}^{EX}_{D,k}$	$\dot{E}^{AV}_{D,k}$	$\dot{E}^{UN}_{D,k}$	$\dot{E}^{EN}_{D,k}$		$\dot{E}^{EX}_{D,k}$	
									$\dot{E}^{AV,EN}_{D,k}$	$\dot{E}^{UN,EN}_{D,k}$	$\dot{E}^{AV,EX}_{D,k}$	$\dot{E}^{UN,EX}_{D,k}$
CC	1575.7	401.1	20.8	401.1	337.8	63.3	33.9	367.2	14.2	324	19.7	43.6
WSPSH	1592.2	179.6	4.26	243.8	217.9	26.0	40.4	203.5	37.2	181	3.13	22.8
FRH	1593.5	3.84	3.04	13.9	12.3	1.56	6.21	7.64	5.48	6.81	0.73	0.83
FSH	1596.0	3.47	0.52	11.5	10.2	1.33	4.07	7.45	3.60	6.60	0.47	0.86
PRH	1593.1	5.13	3.37	29.1	25.9	3.12	12.1	17.0	10.8	15.1	1.25	1.87
ECON	1596.2	7.44	0.26	16.1	14.0	2.13	3.28	12.8	2.81	11.1	0.47	1.66
APH	1552.5	8.17	44.0	21.6	19.4	2.25	10.6	11.0	9.49	9.87	1.10	1.15
HPT1	1571.0	0.00	25.5	10.9	9.90	1.00	1.43	9.47	1.30	8.60	0.13	0.87
HPT2	1588.4	0.00	8.14	3.46	3.03	0.43	1.26	2.20	1.15	1.88	0.11	0.32
IPT1	1586.4	0.00	10.1	3.80	3.63	0.17	2.01	1.79	1.94	1.69	0.07	0.10
IPT2	1588.6	0.00	7.94	3.04	2.68	0.36	1.35	1.70	1.22	1.46	0.13	0.23
LPT1	1588.7	0.00	7.84	3.06	2.78	0.28	1.09	1.97	1.05	1.74	0.04	0.24
LPT2	1590.5	0.00	5.97	2.37	2.13	0.24	1.02	1.35	0.97	1.16	0.05	0.19
LPT3	1589.9	0.00	6.56	2.63	2.31	0.31	0.66	1.96	0.58	1.73	0.08	0.23
LPT4	1565.9	0.00	30.6	12.7	11.5	1.27	6.41	6.32	5.77	5.69	0.64	0.63
LPT5	1575.0	0.00	21.5	8.98	7.84	1.14	1.79	7.19	1.57	6.28	0.23	0.91
COND	1596.5	27.3	0.00	27.3	22.0	5.31	–	–	–	–	–	–
CDP	1596.1	0.00	0.36	0.15	0.09	0.07	0.06	0.09	0.03	0.05	0.03	0.04
H8	1595.8	1.21	0.73	1.34	1.18	0.16	0.18	1.15	0.16	1.02	0.03	0.14
H7	1595.8	1.56	0.71	1.67	1.21	0.46	0.23	1.44	0.04	1.17	0.19	0.27
H6	1595.3	0.83	1.19	0.90	0.61	0.29	0.16	0.74	0.04	0.57	0.12	0.17
H5	1594.3	2.99	2.16	3.02	2.18	0.84	0.34	2.68	−0.01	2.19	0.35	0.49
DA	1595.6	2.98	0.89	2.83	1.79	1.04	0.32	2.50	−0.06	1.85	0.38	0.65
FP	1590.1	0.00	6.41	2.22	1.60	0.62	1.04	1.18	0.74	0.86	0.30	0.32
H3	1594.6	3.00	1.88	3.03	2.36	0.67	0.34	2.69	0.13	2.22	0.21	0.46
H2	1595.2	2.08	1.28	2.37	1.57	0.80	0.30	2.07	−0.03	1.60	0.33	0.47
H1	1594.3	1.33	2.16	1.55	1.17	0.38	0.21	1.33	0.05	1.12	0.16	0.22
ST	1585.4	0.00	11.0	4.92	3.01	1.91	2.19	2.73	1.34	1.67	0.85	1.06
G	1572.6	0.00	23.9	10.2	10.2	0.01	5.49	4.73	5.49	4.73	0.00	0.00

[a] This result is based on the reasonably simplified overall system, where the configuration of the boiler subsystem is in accordance with Fig. 2 and all the pipelines in the turbine subsystem shown in Fig. 1 are removed.

cantly. All the exergy destruction within G is endogenous. Nearly 10% of exergy destructions of turbine stages and components involved in the boiler subsystem are exogenous, while that ratio of the regenerative subsystem almost reaches 30%, which indicates that the effect of the system topology contributes largely to their exergy destructions. The components in the boiler subsystem have large absolute exogenous exergy destruction (a total value of 100 MW), meaning that their performances are significantly affected by the irreversibilities occurring in the components of the turbine subsystem.

The real potential for improving a component is not fully revealed by its total exergy destruction but by its avoidable part. A large part (35–50%) of the exergy destruction within FRH, FSH and PRH and APH is avoidable. Due to chemical reactions, most of the exergy destruction (367 MW) within CC is unavoidable in comparison with the avoidable part (34 MW). In addition, less than 20% of the exergy destruction within WSPSH and ECON can be avoided.

A stable 30–50% of exergy destruction of turbo-machines can be generally avoided, while the percentage of the feedwater preheaters remain below 20%. Since the work is pure exergy and even a slight change of the efficiency of turbo-machinery contributes largely to FC, more attention should be directed toward the efficiency improvement of turbines, pumps and fans.

Most of the avoidable exergy destructions within the heating surfaces, turbine stages and G are endogenous; therefore, the improvement measurements for these components should be concentrated on the components themselves. However, the combustion process has an avoidable/exogenous exergy destruction of nearly 20 MW and, thus, its performance enhancement should include also the irreversibility reductions of other components. Additionally, due to the fact that the exogenous exergy destruction contributes over 70% of the avoidable part within the regeneration subsystem, improving feedwater preheaters can be more efficiently realized at the subsystem level.

It should be noted that there are no contradictions between the discussions of the fuel-savings potentials and the advanced exergy analysis. The former concentrates on the influence of each component on the overall FC, while the latter focuses on the energy-savings potential of the considered component itself.

Another point which should be mentioned is that when we discuss the fuel-saving potentials and the advanced exergy analysis, the steam conditions, i.e. main and reheat steam temperatures and main steam pressure, are considered as fixed, while for the comparisons of the USC unit with SUB units the steam conditions are different. That is why the comparisons show that the system improvement of the USC unit mainly comes from the reduction of the exergy destruction within the boiler.

5.6. Sensitivity analysis

The dependencies of the overall exergetic efficiency ε_{tot} on key parameters, as shown in Fig. 8, were investigated. The black dot with denotation BP represents the basic and real conditions of the plant.

Fig. 8a shows that increasing α by 0.1 can contribute to a reduction of ε_{tot} by 0.16 percentage point (PP), due to the greater exergy loss caused by the mass flow increase of exhausted flue gas. For a given α, an increase of ε_{tot} by 1PP requires only a 50 °C decrease of $t_{ex,fg}$, emphasizing that the utilization of the waste heat of flue gas is of great importance.

Fig. 8b illustrates that, for a given t_{ms}, the variation range of ε_{tot} due to the increase of p_{ms} is rather small, and the higher the t_{ms}, the larger the variation. Additionally, an increase of t_{ms} by 50 °C contributes to an increase of ε_{tot} by 1PP. For a given structure of the plant, the variable p_{ms}, $t_{rh,h}$ exerts great impact on ε_{tot} as presented

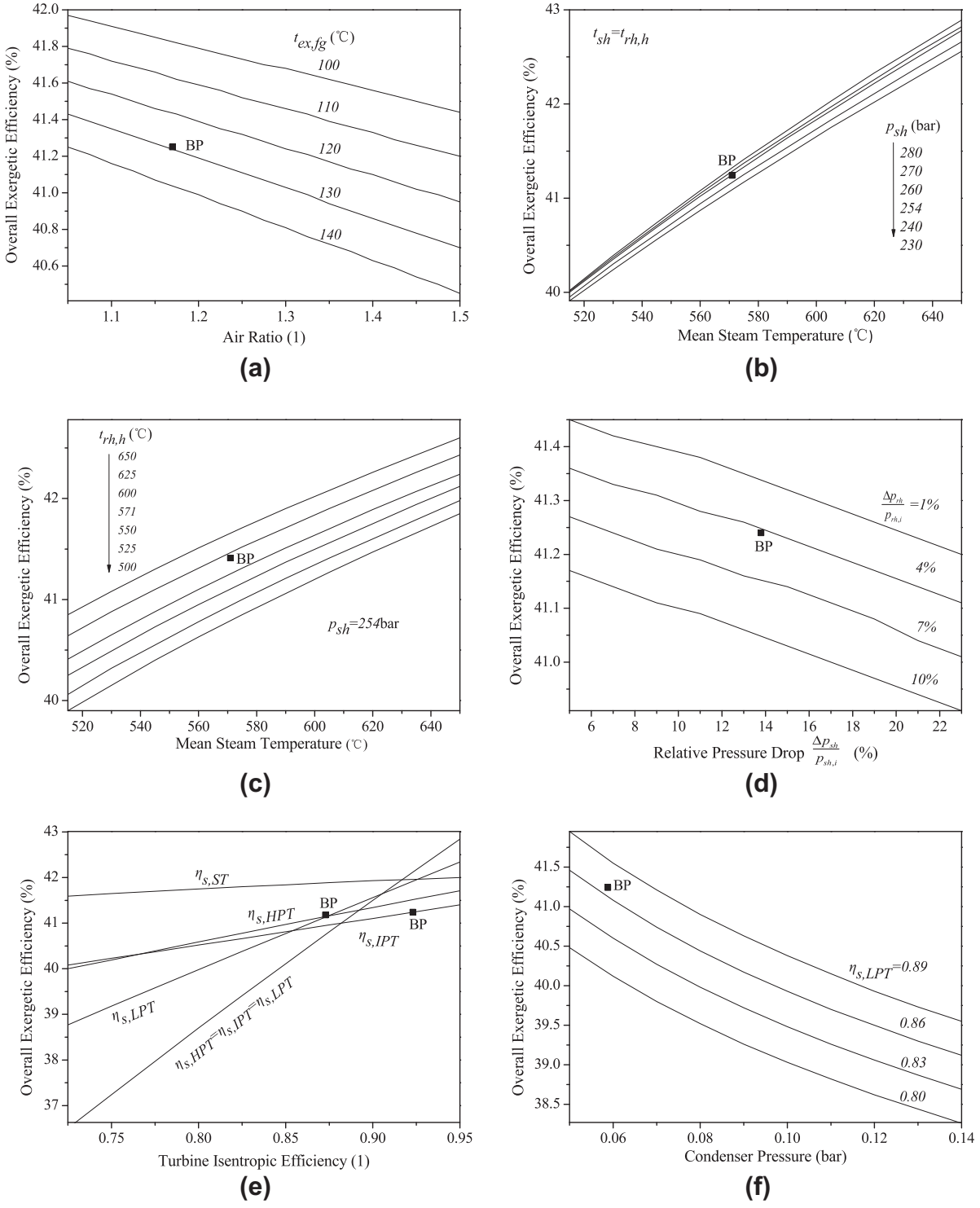

Fig. 8. The dependencies of the overall exergetic efficiency ε_{tot} on key parameters.

in Fig. 8c. In this way, within the permit of metal material, t_{ms} and $t_{rh,h}$ should be kept as high as possible for a better performance.

Fig. 8d displays the influence of pressure drop ratio in reheater, which is almost three times larger than that of the same ratio in steam generator since the latter can be easily compensated by pumping feedwater to a higher pressure in FPs.

Fig. 8e shows that $\eta_{s,LPT}$ is proven to have a greater effect on ε_{tot} due to its highest contribution to P_{tot}. The effects of $\eta_{s,HPT}$ and $\eta_{s,IPT}$ are relatively small and quite similar to each other. In addition, $\eta_{s,ST}$ seems to exert only limited impact on ε_{tot}.

Fig. 8f illustrates the great impact of the p_{COND} on ε_{tot}. An increase in p_{COND} by 0.02 bar can lead to an efficiency drop by almost 0.6PP, emphasizing the importance of keeping p_{COND} as low as possible also from the economics perspectives.

5.7. Improvement strategies

The aforementioned results not only demonstrate where and to what extend can the improvements at both the system and the component levels be obtained, but also suggest the sequence of

improving an individual component or subsystem to fulfill its largest benefits. The enhancement of turbo-machines (including G), turbines, pumps and fans must be given a high priority by focusing on the components themselves. Only when as much as possible the mechanical energy is saved can the improvements of other components be more efficient and practical. Then, the regeneration subsystem may be improved at the subsystem level. At the same time, it would be more beneficial if the waste heat of the boiler exhaust can be cost-effectively utilized. The attempts to reduce FC by improving heating surfaces and combustion tend to bring very limited fuel-saving on the basis of the current design concept for boilers of CP plants. It is also suggested that great profits can be achieved from heat transfer in the boiler subsystem if the conversion mode from the fuel exergy to the flue gas exergy can be accordingly adjusted.

6. Conclusions

This paper presents a comprehensive exergy-based evaluation of a state-of-the-art USC CP plant. The conventional exergy analysis is aiming at quantifying the exergy dissipation within the whole system, while the discussions on the fuel-savings potentials and an advanced exergy analysis reveal the energy-savings potential from different levels. Comparisons with existing SUB units are conducted to show the change of the spatial distribution of exergy destruction and losses. Here, we list some significant conclusions as follows:

(1) The energy-saving potentials for both the overall system and an individual component are not in accordance with the amounts of their exergy destructions. The boiler subsystem has the largest exergy destruction; however, currently, the benefit for FC reduction by its improvement is limited.
(2) Compared with SUB units, the exergy destruction ratios of each subsystem in the USC unit do not diminish homogeneously but only that of boiler reduces significantly, which leads to its efficiency improvement.
(3) The improvement approaches for different components differ quite a lot based on advanced exergy analysis. For instance, efforts on improving turbo-machines should be dedicated to themselves and those of feedwater preheaters should be focused on a subsystem level, while enhancing the combustion process needs more attention for both the process itself and other components.

It is also concluded that the exergy analysis in the case of a steam power plant cannot provide more information on how to

Table A.1
Properties of streams of boiler subsystem, corresponding to Fig. 1.

Sec.	Type[a]	Name[b]	$\dot{m}$ (kg/s)	t (°C)	p (bar)	$\dot{E}_{tot}$ (MW)	Sec.	Type	Name	$\dot{m}$ (kg/s)	t (°C)	p (bar)	$\dot{E}_{tot}$ (MW)
I	I	coal	69.6	25.0	1.0	1621.3	VII	I	fg	661.4	991.1	1.0	470.9
		air	594.1	328.0	1.0	58.1			mwf	532.6	508.0	258.0	750.6
		mwf	511.3	336.0	291.4	248.3			awf1	204.5	435.1	265.2	244.8
	O	fg	646.5	1559.3	1.0	850.0			awf2	511.3	429.4	268.6	597.7
		slag	16.3	600.0	1.0	16.3		O	fg	661.4	837.9	1.0	375.8
		mwf	511.3	405.0	280.7	503.2			mwf	532.6	571.0	254.0	823.0
II	I	fg	646.5	1559.3	1.0	850.0			awf1	204.5	437.8	264.5	247.0
		air	14.9	25.0	1.0	0.0			awf2	511.3	431.0	267.9	601.6
		mwf	511.3	405.0	280.7	503.2	VIII	I	fg	661.4	837.9	1.0	375.8
	O	fg	661.4	1386.6	1.0	740.7			mwf	449.1	455.0	43.3	576.6
		mwf	511.3	421.0	277.1	568.8			awf1	112.7	435.4	263.9	135.3
III	I	fg	661.4	1386.6	1.0	740.7			awf2	511.3	431.0	267.9	601.6
		mwf	511.3	438.2	263.2	619.3		O	fg	661.4	796.5	1.0	351.2
		awf1	306.8	421.0	277.1	341.3			mwf	449.1	480.0	43.0	591.9
		awf2	511.3	426.9	270.6	590.3			awf1	112.7	441.6	263.2	137.9
	O	fg	661.4	1243.3	1.0	639.5			awf2	511.3	431.5	267.2	603.2
		mwf	511.3	479.0	260.0	683.7	IX	I	fg	661.4	796.5	1.0	351.2
		awf1	306.8	426.2	273.6	351.5			awf1	194.1	435.4	263.9	232.8
		awf2	511.3	428.7	269.9	594.9			awf2	511.3	431.5	267.2	603.2
IV	I	fg	661.4	1243.3	1.0	639.5		O	fg	661.4	777.2	1.0	339.9
		mwf	524.7	468.6	260.0	687.0			awf1	194.1	437.3	263.2	234.4
		awf1	57.3	421.0	277.1	63.7			awf2	511.3	434.9	266.6	610.6
		awf2	511.3	428.7	269.9	594.9	X	I	fg	661.4	777.2	1.0	339.9
	O	fg	661.4	1117.9	1.0	554.1			mwf	449.1	313.2	43.9	491.5
		mwf	524.7	516.0	258.0	748.9			awf1	306.8	434.8	264.5	367.1
		awf1	57.3	427.7	273.6	66.0			awf2	511.3	434.9	266.6	610.6
		awf2	511.3	429.4	269.2	597.1		O	fg	661.4	572.6	1.0	228.5
V	I	fg	661.4	1117.9	1.0	554.1			mwf	449.1	455.0	43.3	576.6
		mwf	449.1	480.0	43.0	591.9			awf1	306.8	435.4	263.9	368.1
		awf1	24.5	421.0	277.1	27.3			awf2	511.3	435.4	265.9	612.0
		awf2	511.3	429.4	269.2	597.1	XI	I	fg	661.4	572.6	1.0	228.5
	O	fg	661.4	1009.0	1.0	482.4			mwf	511.3	283.5	293.4	178.8
		mwf	449.1	569.0	42.0	648.2		O	fg	661.4	385.3	1.0	143.0
		awf1	24.5	425.5	273.6	28.0			mwf	511.3	336.0	291.4	248.3
		awf2	511.3	429.4	268.6	597.7	XII	I	fg	661.4	385.3	1.0	143.0
VI	I	fg	661.4	1009.0	1.0	482.4			air	594.1	25.0	1.0	0.7
		mwf	122.7	421.0	277.1	136.5		O	fg	661.4	127.7	1.0	64.3
	O	fg	661.4	991.1	1.0	470.9			air	594.1	328.0	1.0	58.1
		mwf	122.7	435.0	273.6	145.3			AT1	13.4	283.5	293.4	4.7
									AT2	7.9	283.5	293.4	2.8

[a] I – incoming stream; O – outgoing stream
[b] mwf – Main working fluid; fg – flue gas; awf – auxiliary working fluid through pipes of roof (1) and sidewall (2).

Table A.2
Properties of streams of turbine subsystem, corresponding to Fig. 1

No.	$\dot{m}$ (kg/s)	t (°C)	p (bar)	$\dot{E}_{tot}$ (MW)	No.	$\dot{m}$ (kg/s)	t (°C)	p (bar)	$\dot{E}_{tot}$ (MW)
1	532.0	566.0	242.0	818.0	24	532.0	256.5	293.5	155.2
2	35.5	367.2	67.97	42.3	25	532.0	283.5	293.5	186.1
3	448.4	315.1	45.67	492.9	26	35.5	262.0	65.93	10.2
4	48.1	315.1	45.67	52.9	27	83.6	217.8	44.30	16.5
5	448.4	566.0	41.10	644.2	28	103.7	191.2	19.96	15.6
6	20.1	457.0	20.58	24.3	29	26.3	109.1	4.155	1.2
7	25.5	362.9	10.65	25.7	30	39.4	89.6	1.266	1.1
8	27.9	362.9	10.65	28.1	31	56.9	62.6	0.623	0.7
9	375.0	362.9	10.65	378.8	32	70.0	41.5	0.198	0.3
10	26.3	253.6	4.374	20.7	33	27.9	39.7	0.073	3.1
11	13.1	128.8	1.333	7.1	34	30428.5	25.0	1.000	76.0
12	17.4	88.2	0.655	7.3	35	30428.5	30.8	1.000	83.1
13	13.2	60.9	0.208	3.3	36	35.5	365.5	65.93	42.2
14	305.0	35.8	0.059	24.4	37	48.1	313.6	44.30	52.7
15	402.8	35.8	0.059	1.3	38	20.1	456.6	19.96	24.2
16	402.8	35.9	17.24	2.0	39	25.5	362.4	10.12	25.6
17	402.8	57.1	17.24	4.4	40	27.9	362.4	10.12	27.9
18	402.8	84.1	17.24	10.4	41	26.3	253.2	4.155	20.5
19	402.8	103.6	17.24	16.6	42	13.1	128.4	1.266	7.0
20	402.8	142.2	17.24	32.9	43	17.4	86.9	0.623	7.2
21	532.0	180.4	10.12	70.7	44	13.2	59.8	0.198	3.2
22	532.0	185.7	293.5	88.7	45	375.0	362.7	10.44	377.8
23	532.0	212.3	293.5	111.4					

improve the plant efficiency than it is already known. The exergy analysis used in an exergoeconomic evaluation, particularly in an advanced one, provides very useful information on how to reduce the cost of electricity. In fact, the work in this paper is the first step and will continue with an exergoeconomic analysis to provide practical measures for improving coal-fired power plants.

Acknowledgments

The first four authors would like to thank the National Basic Research Program of China 'Tempo-Spatial Distribution of Energy Consumption, Evaluation Method and System Integration for Large-scale Coal-fired Power Generating Unit' (2009CB219801), the National Basic Research Program of China (2011CB710706) and the National Science Fund for Distinguished Young Scholars (51025624) for the financial support.

Appendix A. Thermodynamic properties of streams under real processes

See Tables A.1 and A.2.

References

[1] BP Company, BP statistical review of world energy; 2011. <www.bp.com> [Retrieved 30.06.12].
[2] International Energy Agency, Organisation for economic co-operation and development, World Energy Outlook; 2010. <www.iea.org/Textbase/npsum/weo2010sum.pdf> [Retrieved 30.06.12].
[3] Yang Y, Guo X, Wang N. Power generation from pulverized coal in china. Energy 2010;35(11):4336–48.
[4] Wolde-Rufael Y. Coal consumption and economic growth revisited. Appl Energy 2010;87(1):160–7.
[5] Bai-Chen X, Ying F, Qian-Qian Q. Does generation form influence environmental efficiency performance? An analysis of china's power system. Appl Energy 2012;96(0):261–71.
[6] Huang B, Xu S, Gao S, Liu L, Tao J, Niu H, et al. Industrial test and techno-economic analysis of CO_2 capture in huaneng beijing coal-fired power station. Appl Energy 2010;87(11):3347–54.
[7] Lund H, Hvelplund F, Nunthavorakarn S. Feasibility of a 1400 mw coal-fired power-plant in thailand. Appl Energy 2003;76(1-3):55–64.
[8] Rukes B, Taud R. Status and perspectives of fossil power generation. Energy 2004;29(12-15):1853–74.
[9] Espatolero S, Cortos C, Romeo LM. Optimization of boiler cold-end and integration with the steam cycle in supercritical units. Appl Energy 2010;87(5):1651–60.
[10] Bugge J, Kjaer S, Blum R. High-efficiency coal-fired power plants development and perspectives. Energy 2006;31(10-11):1437–45.
[11] Beer JM. High efficiency electric power generation: the environmental role. Progress Energy Combust Sci 2007;33(2):107–34.
[12] European AD700 project, <https://projectweb.elsam-eng.com/AD700/default.aspx>. [accessed 25.10.12].
[13] Fukuda Y. Development of advanced ultra supercritical fossil power plants in japan: materials and high temperature corrosion properties. Mater Sci Forum 2010;696:236–41.
[14] Gandy D, Shingledecker J, Viswanathan R. (Eds.). Advances in material technology for fossil power plants. Proceedings from the sixth international conference. August 31–September 3, 2010, Santa Fe, New Mexico, USA, Electric Power Research Institute, Inc.; 2011.
[15] Weitzel P. Steam generator for advanced ultra-supercritical power plants 700 to 760c. In: ASME 2011 power conference. Colorado (USA): Denver; 2011.
[16] Bahadori A, Vuthaluru HB. Estimation of potential savings from reducing unburned combustible losses in coal-fired systems. Appl Energy 2010;87(12):3792–9.
[17] Tan H, Niu Y, Wang X, Xu T, Hui S. Study of optimal pulverized coal concentration in a four-wall tangentially fired furnace. Appl Energy 2011;88(4):1164–8.
[18] Wang D, Bao A, Kunc W, Liss W. Coal power plant flue gas waste heat and water recovery. Appl Energy 2012;91(1):341–8.
[19] Moran MJ. Availability analysis: a guide to efficient energy use. ASME Press; 1989.
[20] Moran MJ, Shapiro HN. Fundamentals of engineering thermodynamics. John Wiley; 1992.
[21] Kotas TJ. The exergy method of thermal plant analysis. Boston (London): Butterworths; 1985.
[22] Szargut J, Morris DR, Steward FR. Exergy analysis of thermal, chemical, and metallurgical processes. Hemisphere Publishing Corporation; 1988.
[23] Bejan A, Tsatsaronis G, Moran M. Thermal design and optimization. John Wiley & Sons; 1996.
[24] Lazzaretto A, Tsatsaronis G. Speco: a systematic and general methodology for calculating efficiencies and costs in thermal systems. Energy 2006;31(8-9):1257–89.
[25] Tsatsaronis G. Design optimization using exergoeconomics. In: Thermodynamic optimization of complex energy systems. Kluwer Academic Publishers.; 1999.
[26] Horlock JH, Young JB, Manfrida G. Exergy analysis of modern fossil-fuel power plants. J Eng Gas Turb Power 2000;122(1):1–7.
[27] Dincer I, Al-Muslim H. Thermodynamic analysis of reheat cycle steam power plants. Int J Energy Res 2001;25(8):727–39.
[28] Sengupta S, Datta A, Duttagupta S. Exergy analysis of a coal-based 210 mw thermal power plant. Int J Energy Res 2007;31(1):14–28.
[29] Aljundi IH. Energy and exergy analysis of a steam power plant in jordan. Appl Therm Eng 2009;29(2-3):324–8.
[30] Wang J, Dai Y, Gao L. Exergy analyses and parametric optimizations for different cogeneration power plants in cement industry. Appl Energy 2009;86(6):941–8.
[31] Ray T, Datta A, Gupta A, Ganguly R. Exergy-based performance analysis for proper om decisions in a steam power plant. Energy Convers Manage 2010;51(6):1333–44.

[32] Suresh M, Reddy K, Kolar AK. Ann-ga based optimization of a high ash coal-fired supercritical power plant. Appl Energy 2011;88(12):4867–73.
[33] Tsatsaronis G, Park M. On avoidable and unavoidable exergy destructions and investment costs in thermal systems. Energy Convers Manage 2002;43(9-12):1259–70.
[34] Cziesla F, Tsatsaronis G, Gao Z. Avoidable thermodynamic inefficiencies and costs in an externally fired combined cycle power plant. Energy 2006;31(10-11):1472–89.
[35] Tsatsaronis G, Morosuk T. A general exergy-based method for combining a cost analysis with an environmental impact analysis: Part ii – application to a cogeneration system. In: ASME conference proceedings; 2008. p. 463–69 [48692].
[36] Tsatsaronis G, Morosuk T. A general exergy-based method for combining a cost analysis with an environmental impact analysis: Part i – theoretical development. In: ASME conference proceedings; 2008. p. 453–62 [48692].
[37] Tsatsaronis G. Recent developments in exergy analysis and exergoeconomics. Int J Exergy 2008;5(5):489–99.
[38] Kelly S. Energy system improvements based on endogenous and exogenous exergy destruction, Ph.D. thesis, Technische Universitat Berlin; 2008.
[39] Kelly S, Tsatsaronis G, Morosuk T. Advanced exergetic analysis: approaches for splitting the exergy destruction into endogenous and exogenous parts. Energy 2009;34(3):384–91.
[40] Morosuk T, Tsatsaronis G. Advanced exergy analysis for chemically reacting systems – application to a simple open gas-turbine system. Int J Thermophys 2009;12:105–11.
[41] Morosuk T, Tsatsaronis G. Advanced exergetic evaluation of refrigeration machines using different working fluids. Energy 2009;34(12):2248–58.
[42] Tsatsaronis G, Morosuk T. Advanced exergetic analysis of a novel system for generating electricity and vaporizing liquefied natural gas. Energy 2010;35(2):820–9.
[43] Boyano A, Blanco-Marigorta A, Morosuk T, Tsatsaronis G. Steam methane reforming system for hydrogen production: advanced exergetic analysis. Int J Thermodyn 2012;15(1):1–9.
[44] Wang L, Yang Y, Morosuk T, Tsatsaronis G. Advanced thermodynamic analysis and evaluation of a supercritical power plant. Energies 2012;5(6):1850–63.
[45] Cziesla F, Tsatsaronis G. Thermoeconomics. In: Encyclopedia of physical science and technology. Academic Press; 2001.
[46] Tsatsaronis G. Strengths and limitation of exergy analysis. In: Thermodynamic optimization of complex energy systems. Kluwer Academic Publishers.; 1999.
[47] Tsatsaronis G, Winhold M. Thermoeconomic analysis of power plants. In: Final Report EPRI AP-3651, RP 2029-8, electric power research institute, Palo Alto, CA, USA; August 1984.
[48] Ahrendts J. Reference states. Energy 1980;5(8–9):666–77.
[49] EBSILON Professional 10 by STEAG Energy Services GmbH. Germany. <www.ebsilon.com> [accessed 25.10.12].
[50] Hebei Xingtai Power, Centralized Control Procedure of Xingtai 220 MW subcritical unit (in Chinese). <www.docin.com/p-362416807.html> [Retrieved 1.12.12].
[51] China Guodian Corporation, Centralized Control Procedure of Hongyanchi 330 MW subcritical unit (in Chinese). <www.docin.com/p-407762020.html> [Retrieved 1.12.12].
[52] Shenhua Guohua Power, Centralized control procedure of Taishan 660 MW subcritical unit (in Chinese). <www.docin.com/p-260987124.html> [Retrieved 1.12.12].